41. Barth, C. A., Rusch, D. W., Thomas, R. C., Mount, G. R., Rottmann, G. J., Thomas, G. E., Sanders, R. W. and Lawrence, G. M., *Geophys. Res. Lett.*, 1983, **10**, 231.
42. Farman, J. C., Gardiner, R. G. and Shanklin, J. D., *Nature*, 1985, **315**, 267.
43. Komhyr, W. D., Grass, R. A. and Leonard, R. K., *Geophys. Res. Lett.*, 1986, **13**, 12.
44. Stolarski, R. S., Krueger, A. J., Schoeberl, M. R., McPeters, M. G., Newman, R. A. and Alpert, J. C., *Nature*, 1986, **322**, 808.
45. McIntire, M., NASA Polar Ozone Workshop, Abstracts, 1988, p. 221.
46. McCormick, M. P., Steele, H. M., Hamill, P., Chu, W. and Swissler, T. I., *J. Atmos. Sci.*, 1982, **39**, 1387.
47. Crutzen, P. J. and Arnold, F., *Nature*, 1986, **324**, 651.
48. Hofmann, D. L. and Solomon, S., *J. Geophys. Res.*, 1989, **94**, 502.
49. McElroy, M. B., Salawich, R. J., Wofsy, S. C. and Logan, J. A., *Nature*, 1986, **321**, 759.
50. Anderson, J. G., Brune, W. H., Lloyd, S. A. and Toohey, D. W., *J. Geophys. Res.*, 1989, **91**, 11480, ALOE special issue.
51. Anderson, J. G., Brune, W. H. Proffit, M. J., Starr, W., Starr, K. R. and Chan, K. R., NASA Polar Ozone Workshop, Abstracts, 1988, p. 143.
52. Molina, M. J., Tso, R. J. and Wang, F. C. W., NASA Polar Ozone Workshop, Abstracts, 1988, p. 251.
53. Stolarski, R. S., personal communication.
54. Bhartia, P. K., Taylor, S. and Fleig, A. J., Proceedings of the Quadrennial Ozone Symposium, 1988, Göttingen, FRG, (ed. Bojkov, R. D. and Fabian, P.), Deepak Publ., Hampton VA, 1989.
55. Dütsch, H. U., *J. Atm. Terr. Phys.*, 1992, **54**, 485.
56. Dütsch, H. U. and Staehelin, J., *Planet. Space Sci.*, 1989, **37**, 158.
57. Mateer, C. L. and DeLuisi, J. J., *J. Atm. Terr. Phys.*, 1992, **54**.
58. Dütsch, H. U. and Staehelin, J., *J. Atm. Terr. Phys.*, 1992, **54**, 557.
59. Stolarski, R. S., Bloomfield, P., McPeters, R. D. and Herman, J. R., *Geophys. Res. Lett.*, 1991, **18**, 1015.
60. WMO/UNEP Scientific Assessment of Stratospheric Ozone-1991, Executive Summary, 1991.
61. Turco, R., Plumb, A. and Condon, E., *Geophys. Res. Lett.*, 1990, **17**, 313.
62. Newman, R. P., Stolarski, R. S., Schoeberl, M., Lait, L. R. and Krueger, A. J., *Geophys. Res. Lett.*, 1990, **17**, 317.
63. Entzian, G., Grasnick, K. H., Feister, U., Wege, K. and Kohler, U., XX General Assembly, IUGG, Vienna, 1991, Abstracts.
64. Toohey, D. W., Brune, W. H., Chan, K. R. and Anderson, J. G., *Geophys. Res. Lett.*, 1991, **18**, 21.
65. Tolbert, M. A., Rossi, M. C. and Golden, D. M., *Geophys. Res. Lett.*, 1988, **15**, 847.
66. NASA, UARS, 1989, illustrated description.

# Laboratory studies of the photochemistry of ozone

**R. P. Wayne**

Physical Chemistry Laboratory, South Parks Road, Oxford, OX1 3QZ, UK

## Introduction

Ozone is a minor constituent of the earth's atmosphere, but one that plays a disproportionately important part in atmospheric physics and chemistry[1]. Atmospheric ozone absorbs solar radiation strongly, and consequently influences the temperature structure and dynamics of the stratosphere. There is a powerful interrelation between circulation and other meteorological phenomena, the radiation field and stratospheric chemistry. One outstanding feature, of course, is the relationship between the absorption spectrum of ozone and the protection of living organisms from unattenuated solar ultraviolet radiation. Because ozone has a positive enthalpy of formation, reactions involving the molecule have a tendency to be exothermic and thermodynamically favoured, and reaction rates are often high. If ozone absorbs radiation, the energy of the system is further elevated and yet other reactions become accessible. In particular, at wavelengths shorter than about 310 nm, ozone is photodissociated by ultraviolet radiation, and two excited fragments are formed

$$O_3 + h\nu \rightarrow O(^1D) + O_2(^1\Delta_g) \quad (1)$$

in a large proportion of the photodissociation events. The excited atomic fragment is able to participate in key reactions such as

$$O(^1D) + H_2O \rightarrow OH + OH \quad (2)$$

$$O(^1D) + CH_4 \rightarrow OH + CH_3 \quad (3)$$

$$O(^1D) + N_2O \rightarrow NO + NO \quad (4)$$

which generate radicals, especially OH in the stratosphere and the troposphere, and NO in the stratosphere. With excited atomic oxygen the reactions are fast, but with ground-state oxygen they are too slow to be of importance. The radicals themselves are of paramount significance in the atmosphere. Indeed, in daytime tropospheric chemistry, many transformations involve the OH radical, and it is difficult to postulate sources of this radical that do not start with the photodissociation of ozone.

Not only is the atomic fragment of the ultraviolet photodissociation of ozone electronically excited, but so

is the molecular moiety. The strongest feature of the terrestrial dayglow is the 'infrared atmospheric band' at $\lambda = 1270$ nm, resulting from the $O_2(^1\Delta_g \rightarrow {}^3\Sigma_g^-)$ transition, and the upper state is excited mainly through photodissociation of $O_3$ in reaction (1). Indeed, if the efficiency of excitation is known, measurements of airglow intensity can be used for the remote monitoring of atmospheric ozone concentration; this method is used, for instance on the SME satellite[2,3].

The simple examples just presented make it evident that a knowledge of the efficiency of the production of excited species in the photodissociation of ozone is a prerequisite in the quantitative interpretation of many aspects of atmospheric chemistry. The information needed can only come from laboratory experiments. Ozone photochemistry has been studied in the laboratory for well over a century and aeronomers and atmospheric chemists have been able to apply the results of the experiments to their own endeavours. However, there is also a great fundamental interest in the physical chemistry of ozone photochemistry that has prompted investigation of the details of dissociation at increasingly sophisticated levels. The development of time-resolved methods, together with direct identification of the fragments, has allowed successively more detailed examination of the dynamics of dissociation. In general, the effort has been directed towards investigation of the energy and angular distributions of the fragments as they are born, and experiments on the femtosecond timescale have been applied to investigate the molecule immediately after it has absorbed radiation and as it is in the process of falling apart[4,5]. It is becoming increasingly evident that studies of this kind are not only of interest to physical chemists, but that they may also be of considerable relevance in atmospheric science. Even at the level of the electronically excited states of atomic and molecular oxygen with which this introduction started, it is clear that the systems concerned are far from thermodynamic equilibrium. Vibrationally excited species derived from ozone photodissociation may also be important, even in the stratosphere[5]. Interpretation of ozone chemistry in the mesosphere and thermosphere certainly requires explicit state-to-state dynamic information because the distribution of energy amongst electronic, vibrational, rotational and translational modes can only be assessed if the nascent distributions are known. In addition, the more detailed our understanding of the phenomenon of photodissociation, the more reliable will be the predictions of behaviour under conditions not accessible in the laboratory, but which may be relevant to atmospheric studies. An understanding of chemical dynamics at the molecular level often provides a key to the understanding of behaviour of bulk systems[6].

In this review, developments in the study of ozone photochemistry are surveyed First, the important spectral transitions in ozone are described and some information is presented on the electronic states involved in ozone photochemistry. Subsequently, the photodissociation itself is considered, first in terms of the electronic states of the products, and then in terms of vibrational excitation in the molecular fragment. Finally, the dynamics of dissociation are considered at the most detailed level for which data are available. More extensive, but less up-to-date, reviews of ozone photochemistry have been published elsewhere[7,8].

## Spectroscopy and electronic states of ozone

A full and critical survey of ozone spectroscopy has been prepared by Steinfeld *et al.*[9]; a summary only is provided here.

Four distinct systems are recognized for the optical absorption of ozone in the near infrared to conventional ultraviolet regions of the spectrum. The longest wavelength electronic absorption is that of the Wulf system in the near infrared, which blends into the Chappuis bands in the visible region. The Huggins bands appear in the near ultraviolet, with an inferred[10] (but not observed) origin at $\lambda = 368.7$ nm. All these three systems consist of diffuse bands. At wavelengths somewhat longer than 300 nm, the Huggins bands are replaced by the Hartley continuum. This system is the strongest of all, with a peak absorption near $\lambda = 250$ nm.

The Wulf bands involve the $1^1A_2 \leftarrow 1^1A_1$ transition, which is not allowed for vibrationally unexcited species, but which becomes vibronically allowed in the asymmetric stretching mode. The most recent[11] analysis of the absorption spectra near 1 $\mu$m suggests that the lowest point on the $^1A_2$ surface lies at $9990 \pm 70$ cm$^{-1}$ or 1.24 eV, above the minimum of the $^1A_1$ ground state. The Chappuis bands lie at somewhat higher energies. Vaida *et al.*[12] have suggested, on the basis of structure seen in condensed-phase spectra, that the upper level of these bands is the $^1A_2$ state. However, this conclusion is disputed[11], and the consensus is that the $1\,^1B_1 \leftarrow 1\,^1A_1$ transition gives rise to the Chappuis bands. The observed vibrational spacing is rather larger than the prediction of Hay and Dunning[13].

Hay *et al.*[14] assign the Hartley band to the $1\,^1B_2 \leftarrow 1\,^1A_1$ transition, and the shape of the continuum arises largely from a symmetric stretching progression[14-17], dissociation along the asymmetric stretching mode being responsible for the vibrational broadening that produces the continuum[4,13,14]. One of the uncertainties concerning the photodissociation of ozone is the source of the structure in the centre of the Hartley band[18]. Johnson and Kinsey[18] have shown, by Fourier transformation of the absorption spectrum, that the structure corresponds to recurrent features in the autocorrelation function in the first hundreds of

femtoseconds following absorption. Unstable periodic or nearly periodic orbits in the photodissociation dynamics (see section on 'rotational energies and the dissociating molecule') are thought to give rise to these time-dependent features. Subsequent effort has recently been directed to a theoretical interpretation of the recurrences[19–22].

A locally bound region on the $1^1B_2$ surface may be responsible[10] for the Huggins bands, although there is also speculation[23] that the $2^1A_1$ state may be involved. Bands arising from odd $\nu_3$ appear in the Huggins system; such bands should be forbidden if the molecule has $C_{2v}$ symmetry. However, recent experiments[24] on the excitation of fluorescence suggest that the upper state of the Huggins system is, indeed, effectively the $1^1B_2$ state, but with $C_s$ symmetry (as predicted[13–15,25] by calculation) rather than $C_{2v}$ symmetry. The fluorescence excitation studies employed jet cooling of the ozone to ca. 3 K to remove rotational congestion, and partial resolution of rotational structure was possible that led both to the identification[10,24] of the upper state in the Huggins system and to an upper bound for its lifetime[24] of 3.6 ps.

Considerable theoretical effort[13,22,25–31] has gone into calculating the energies and properties of electronically excited states and potential energy surfaces for ozone that assist in understanding the spectroscopy, photochemistry and dissociative pathways. A great deal of attention[31] has been paid recently to sophisticated treatments of electron correlation in ozone, especially in the ground state. Incidentally, this type of calculation[32] shows that the cyclic ($D_{3h}$) form of ozone lies at energies above the dissociation limit of the open form to ground-state fragments.

Figure 1 shows some potential energy curves for singlet states of $O_3$ calculated recently[25] by *ab initio* methods. The curves represent sections through the potential surfaces in which one bond distance and the bond angle are held constant at their ground-state equilibrium values. The correlation of these states with $O_2+O$ states is indicated, and is relevant to the discussion to be presented in the next section.

Experimental evidence for bound excited states of ozone is rather sparse. High resolution inelastic scattering data have been used to infer[33] information about singlet and triplet states at relatively high energies (>3.75 eV). Shi and Barker[34] have studied time-resolved infrared fluorescence following laser photoexcitation of $O_3$ in the Hartley band. Several bands are observed, of which one, at $\lambda \simeq 1{\cdot}9\ \mu m$, may result from a triplet state of $O_3$. The only other direct observation of low-lying triplet excited states is that of Swanson and Celotta[35], who observed a broad peak near 1.65 eV in an electron impact study for a scattering angle of 90 degrees, where spin-forbidden transitions should be most prominent. The $1^3B_1$ state is accessible,

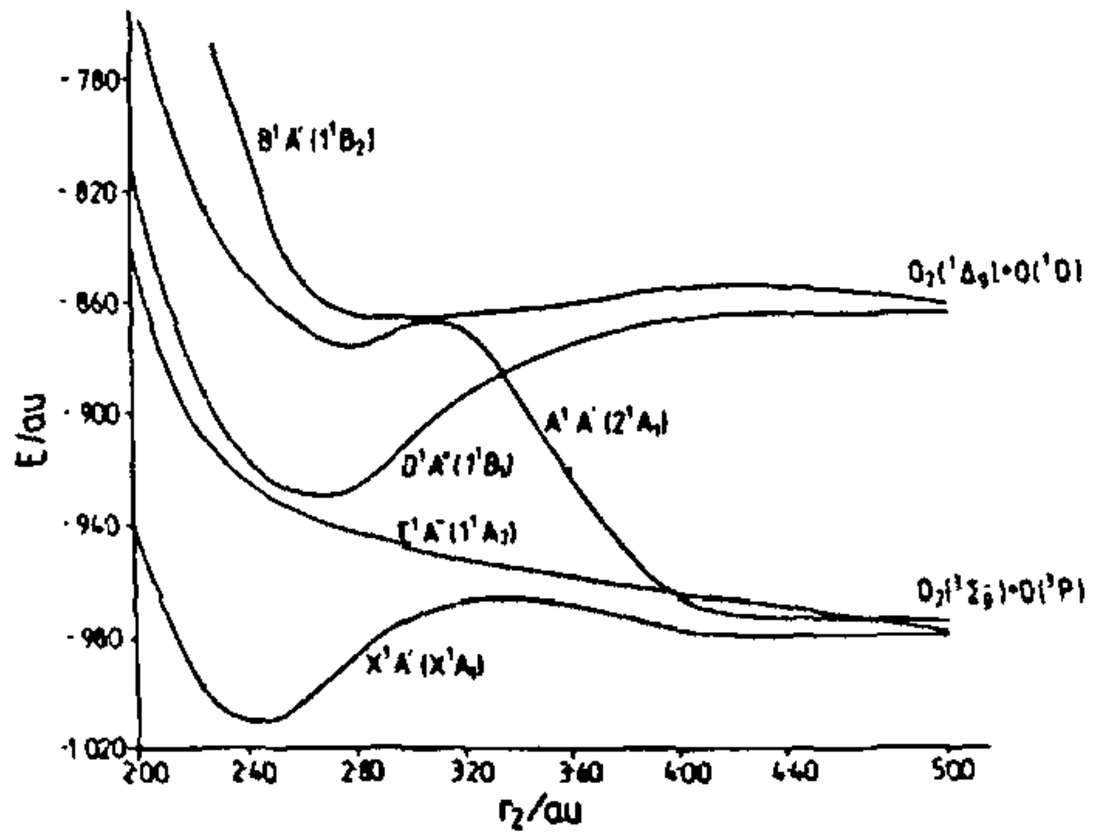


**Figure 1.** Potential energy curves[25] for some singlet states of ozone. The energies are shown as a function of one O–O bond distance with the other inter-bond distance (2.413 au) and the bond angle (116.8°) held at the ground-state equilibrium values. The electronic states are given first for $C_s$ symmetry, and then in parentheses for $C_{2v}$ symmetry of the molecule.

although the observed[35] features may include contributions from the lower triplets ($1^3B_2$, $1^3A_2$). McGrath and co-workers[36] have reported an absorption transient following irradiation of ozone in the visible region by a dye-pumped flash system. Enhanced absorption in the ultraviolet region was observed, at a peak wavelength of 320 nm. Arguments were presented to support the assignment of the absorption to electronically excited ozone, probably in the $1^1A_2$ state, with a radiative lifetime of about 4 ms. Circumstantial corroboration comes from the experiments of Shi and Barker[34] and von Rosenberg and Trainor[37], who observed infrared emission on the recombination of O with $O_2$. Most of the emission results from vibrational transitions in ground-state ozone, but part of the chemiluminescence may derive from electronically excited ozone. Wraight[38] suggests that the upper state involved is the $1^1A_2$, and provides explanations for why this state should be populated. Further experiments by Bair and co-workers[39,40] on the recombination of O with $O_2$ seem to be consistent with more than 60 per cent of the ozone first formed being electronically excited, probably in the $^3B_2$ state, and the same state is invoked by Ramirez *et al.*[41] as one of the routes to formation of $O_3$ in the pulse radiolysis of oxygen. Nevertheless, it seems at present that the identification of the excited states in the enhanced absorption[36], infrared emission[34,37] or kinetic[39–41] experiments is far from certain.

## Product electronic states in ozone photolysis

Ozone has a peculiarly rich photochemistry partly in consequence of the rather weak energy of the $O_2$ O

bond (just over 106 kJ $mol^{-1}$ or 1 eV). Both atomic and molecular oxygen have several accessible excited states. Table 1 shows some of the thermochemical thresholds, expressed as wavelengths in nm, for different dissociation channels. The experimental evidence shows that absorption in the Chappuis bands of the visible region of the spectrum leads to the formation of *two* triplet, ground state, fragments, while in the strong part of the Hartley band, at $\lambda < 300$ nm, the products are mainly—but not exclusively—the *two* singlets shown by the table to be energetically accessible ($O_2(^1\Delta_g) + O(^1D)$). Circumstantial evidence first led to these conclusions[42–44]; other indirect and direct identifications of the products of photolysis have subsequently become available, and will be described later. At wavelengths shorter than 237 nm, $O(^1S)$ becomes an energetically possible product, although experiments[45] in the wavelength range 170–240 nm show that the $^1S$ state atom is not produced to a significant extent. Indeed, at $\lambda = 157.6$ nm, about half the ozone molecules fragment to $O(^1D) + O_2(^1\Sigma_g^+)$; the remainder of the ozone dissociates via a new route to O + O + O (ref. 46).

The experimental data thus show that absorption of a sufficiently energetic photon does not guarantee that an energetically accessible route will in fact be followed, although thermodynamics, as embodied in Table 1, may impose a limiting constraint on the dissociation channels. Other conditions may also need to be satisfied for the actual occurrence of fragmentation by any given pathway. In particular, reactions are generally efficient only if they proceed *adiabatically*; that is, if a single continuous potential energy surface connects products with reactants. Of the correlation or conservation rules that are based on this concept, the important ones in the decomposition of ozone are those concerned with spin and with orbital symmetry. For example, if the O and $O_2$ fragments of the dissociation are to correlate with a singlet excited state of $O_3$, the spin-conservation argument runs that both fragments must be singlets or both must be triplets. With this rule imposed, some of the pairs of products suggested by Table 1 are excluded. Figure 1 illustrates more fully the correlations between different singlet states of $O_3$ and the states of $O + O_2$. A certain amount of caution is needed in applying the spin and other conservation rules. Spin-orbit coupling can relax the rigour with which the $\Delta S = 0$ rule must be applied in both optical and radiationless transitions; the excitation process could also occur without conservation of spin, and the subsequent dissociation might be non-adiabatic. The other point that should be made is that the rules show *excluded* possibilities rather than permitted ones. We shall return several times later to consideration of the validity of the spin conservation rule.

**Table 1.** Thermochemical thresholds (expressed as wavelengths in nm) for photodissociation of ozone to different electronic states of the products.

| | Molecule | | | | |
|---|---|---|---|---|---|
| Atom | $O_2(^3\Sigma_g^-)$ | $O_2(^1\Delta_g)$ | $O_2(^1\Sigma_g^+)$ | $O_2(^3\Sigma_u^+)$ | $O_2(^3\Sigma_u^-)$ |
| $O(^3P)$ | 1180 | 612 | 463 | 230 | 173 |
| $O(^1D)$ | 411 | 310 | 267 | 168 | 136 |
| $O(^1S)$ | 237 | 199 | 181 | 129 | 109 |

As emphasized in the introduction, $O(^1D)$ drives chemical transformations of great importance in the stratosphere and troposphere. Photolysis of ozone by ultraviolet radiation is the source of the excited atomic oxygen, so that a knowledge of the efficiency of $O(^1D)$ production is vital to a quantitative understanding of much of atmospheric chemistry. The wavelengths indicated in Table 1 would be the absolute limits for the formation of any particular product pair, were it not for the possible utilization in dissociation of internal energy in the molecule. Vibrational and rotational energy can, in fact, contribute towards the total energy necessary for dissociation, so that the onset of participation of a channel does not have to be a step-function of wavelength, and it may be a function of temperature. One particularly significant photochemical region is the long-wave tail of the Hartley–Huggins bands. In this region, solar intensity rises rapidly, but is accompanied by a sharp decrease in absorption cross section. The variation with wavelength of quantum yield for $O(^1D)$ production thus has a profound effect on the predicted rate of excited atom formation. Many experiments have shown that there is a marked decrease in $\phi(^1D)$ as $\lambda$ increases from 254 nm to 334 nm, the yield being essentially zero at the longer wavelength. At $\lambda = 310$ nm, $\phi(^1D)$ is around 0.1 of its value at $\lambda = 254$ nm. Such behaviour is, at least qualitatively, that expected if photolysis is spin conserved, since, as shown in Table 1, $\lambda = 310$ nm is approximately the thermochemical threshold for formation of two singlet products. Subsequent experiments, both static and those using laser flash photolysis, have greatly refined the early results[47–54].

The absorption spectrum of ozone is temperature-dependent, and vibrational excitation of ozone seems to be responsible for the changes[16,55–57]. The exact form of the $\phi(^1D)$–$\lambda$ curve is also temperature-dependent[58], probably because vibrational excitation can contribute to the total energy available for dissociation of ozone. Moortgat and Kudszus[54] have cast the experimental data for both the wavelength and temperature dependences of $\phi(^1D)$ in an analytical form. With modification for the likely absolute values of $\phi(^1D)$, to be discussed next, the expression is the basis for the quantum yields quoted in current data evaluations[59].

Most measurements of the quantum yields for $O(^1D)$ production at wavelengths around the fall-off region at the energetic threshold (i.e. ca. $\lambda = 310$ nm) have been made relative to those for shorter wavelengths, where the quantum yield has often been assumed to be unity

on the basis of the spin-conservation arguments discussed earlier. Several pieces of information show that the $O(^1D)+O_2(^1\Delta_g)$ channel may not be the only one operating for ozone photolysis at wavelengths shorter than the thermodynamic threshold, although it may be the dominant one.

Two time-of-flight photofragment spectroscopy studies have indicated that the quantum yield for *ground* state, $O(^3P)$, atom formation is about 0.1 at wavelengths around 270 nm. Sparks *et al.*[60] showed that most of the atomic oxygen photofragments can be identified with formation of $O_2(^1\Delta_g)+O(^1D)$, with four peaks corresponding to $v=0$, 1, 2, and 3 in the $O_2$; a broad high energy feature, however, can only result from dissociation in the $O_2(^3\Sigma_g^-)+O(^3P)$ channel, which must contribute roughly 10 per cent to the total dissociation. Fairchild *et al.*[61] reached similar conclusions from their study of the atomic oxygen fragment. More recent experiments of Kinugawa *et al.*[62], using REMPI detection of $O(^3P)$ with laser photolysis of $O_3$ at $\lambda=226$ nm, have also shown that ground-state atomic oxygen is formed, although these experiments addressed primarily details of the fragmentation dynamics (see later) and do not give a quantitative measure of the fraction of dissociation events leading to ground-state products.

Flash photolysis experiments confirm that some of the dissociation proceeds via the triplet channel. Photolysis at $\lambda=248$ nm[63,64] and at $\lambda=266$ nm[65] indicates that about 10 per cent of $O(^3P)$ is formed promptly after the photolytic flash (i.e., in the primary step), while additional $O(^3P)$ builds up subsequently as a result of the secondary reactions anticipated. Wine and Ravishankara[66] have measured $\phi(^1D)$, and obtain a value of 0.9 at $\lambda=248$ nm, in substantial agreement with the interpretation put on the measurements of $\phi(^3P)$. Experiments at wavelengths near the threshold for $O(^1D)$ production suggest[64] that $\phi(^1D)=0.96$ at $\lambda=300$ nm. That is, the quantum yield is apparently higher at the threshold than it is at shorter wavelengths. Brock and Watson[48,65] also find evidence that $\phi(^1D)$ decreases slightly between $\lambda=304$ nm and $\lambda=275$ nm. The trend is even more apparent in relative measurements of $\phi(^1D)$ made by Trolier and Wiesenfeld[67] over the wavelength range 275–325 nm. At wavelengths between 300 and 285 nm, the relative yield stays essentially the same; however, at shorter wavelengths the yield declines, and by $\lambda=274$ nm it has decreased to $0.86\pm0.06$ (relative to unity at the longer wavelengths). Absolute measurements[68] at $\lambda=222$ nm show that $\phi(^3P)=0.13\pm0.02$, and indirect, but absolute, measurements of the yield of $O(^1D)$ suggest a value of $\phi(^1D)=0.87\pm0.04$ at the same wavelength. That is, the *total* yield of atomic oxygen in the $^1D$ and $^3P$ states is confirmed to be unity at this wavelength. A decrease in $\phi(^1D)$ at wavelengths shorter than those near the threshold is not excluded on theoretical grounds, although it is not necessarily predicted, either. The formation of any triplet products in the ultraviolet region is presumably a result of a predissociation from the electronic states that more frequently yield the singlet fragments by direct dissociation. With reference to the potential energy curves[25] of Figure 1, for example, crossing from the $B^1A'$ state first populated by absorption to the $A^1A'$ state could lead to ground-state products. The efficiency of crossing will be determined by the mixing of the electronic states and the velocity of approach to the intersection. The variation of this efficiency with wavelength will thus depend also on the exact energy and geometry of the surfaces. At shorter wavelengths again, quite different behaviour may be expected as new electronic states are populated. As stated earlier, Taherian and Slanger[46] identified a channel leading to three oxygen atoms at $\lambda=157.6$ nm. Evidence exists[68] for the operation of a similar dissociation channel at $\lambda=193$ nm. At this latter wavelength, there appears also to be coproduction of $O(^1D)$ and $O_2(^1\Sigma_g^+)$.

Valentini and co-workers[69,70] have obtained experimental confirmation of the curve-crossing process from the rotational quantum-state distributions in the $O_2(^1\Delta_g)$ fragment of the Hartley band photodissociation of ozone. The experiments themselves, and their interpretation, are discussed in the section 'rotational energies and the dissociating molecule'. It suffices to say here that these experiments provide a way of determining the quantum yield for the triplet channel. Valentini *et al.*[70] find that their results do *not* fit in with a value of $\phi(^1D)$ that is unity at wavelengths near the energetic threshold, but which decreases at shorter wavelengths. Rather, they argue for a constant branching ratio for the singlet channel of 0.89 over the wavelength range 266 to 311 nm. In fact, the apparent constancy of the values of the triplet yield at the longest wavelengths is itself rather puzzling, since most other studies indicate values of $\phi(^3P)$ substantially above 0.11 for $\lambda>308$ nm. One possible explanation is that there is an additional, spin-forbidden, dissociation channel in the long-wavelength tail of the Hartley absorption band. This idea will shortly be explored further.

Although there is enough energy (cf Table 1) for $O_2(^1\Delta_g)$ to be a product of the photolysis of ozone in the Chappuis region, all the available evidence[61,71–74] indicates that excited products are not formed in the visible-region photolysis. That is, spin conservation determines the pathway of photolysis in the visible region of the spectrum. On the other hand, laboratory experiments, described in detail elsewhere[44,75–81], show explicitly that $O_2(^1\Delta_g)$ is the molecular fragment of ozone photolysis in the ultraviolet. Although $O_2(^1\Sigma_g^+)$ could be produced at $\lambda=253.7$ nm (see Table 1), a limit of less than five per cent has been placed[79] on

its excitation efficiency at this wavelength. Absolute calibration for $O_2(^1\Delta_g)$ emission intensities allowed Jones and Wayne[80] to show that the species was formed with an efficiency of $0.83 \pm 0.11$ at $\lambda = 253.7$ nm.

Other experiments confirm that $O_2(^1\Delta_g)$ is a product of photolysis of ozone by ultraviolet radiation. The photofragment spectroscopy experiments[60,61] show energy releases consistent only with the formation of the excited singlet oxygen. Furthermore, the coherent Raman studies[69,70] directly examine the $O_2(^1\Delta_g)$ molecule, and are able to resolve detailed vibrational and rotational structure.

All the experiments that suggest a value for $\phi(O^1D)$ of less than unity for ultraviolet photolysis also imply that the quantum yield for $O_2(^1\Delta_g)$ production will be less than one in the photolysis of ozone. It thus seems that the measurement of $\phi(^1\Delta_g) = 0.83 \pm 0.11$ of Jones and Wayne[80] should be taken at face value. The significance of this conclusion for atmospheric studies is that the production rates of $O_2(^1\Delta_g)$ in the atmosphere must be scaled by the primary quantum yield. One application, for example, where a value of $\phi \simeq 0{\cdot}8 - 0{\cdot}9$ might have an impact is in the derivation of ozone concentrations from airglow intensities in the infrared atmospheric band, $O_2(^1\Delta_g \rightarrow {}^3\Sigma_g^-)$, as applied to data from the SME infrared instrument[2,3].

One further finding upsets the simple idea of spin-conserved photodissociation of ozone giving rise entirely to two singlet or two triplet products with the threshold being set by thermodynamic constraints. This finding concerns the production of $O_2(^1\Delta_g)$ at wavelengths longer than the $\lambda = 310$ nm threshold. The evidence suggests[81-83] that $O_2(^1\Delta_g)$ formation remains efficient at $\lambda = 334$ nm, even though production of $O(^1D)$ no longer occurs. That is, the dissociation appears to be spin forbidden in this weak absorption region. The fragments $O(^3P) + O_2(^1\Delta_g)$ correlate with the $1^3B_1$ and $2^3B_2$ states of ozone; the vertical excitation energy of the $2^3B_2$ state of $O_3$ lies at about[26] 3.27 eV, corresponding to an onset of absorption at $\lambda = 379$ nm. Direct, but forbidden, population of the $2^3B_1$ state might therefore be achieved by the weak optical absorption at $\lambda = 334$ nm. An alternative route to the photolytic fragments that correlate with triplet states of ozone would, of course, be optical absorption in the singlet system, and (forbidden) crossing to the triplet.

Rotational quantum-state populations[70] in the $O_2(^1\Delta_g)$ product of ozone photolysis at the long-wavelength end of the Hartley continuum also suggest that there is a dissociation channel additional to that yielding the $O(^1D) + O_2(^1\Delta_g)$ singlet pair. However, the CARS spectra show no evidence for the appearance of a $O(^3P) + O_2(^1\Delta_g)$ channel, which should be accompanied by changes in rotational and vibrational distributions at the longer wavelengths ($\lambda = 308$–$311$ nm) in these experiments. An alternative possibility for the additional channel is that the $O_2$ is formed in the second, $b^1\Sigma_g^+$ state, for which, unfortunately, a search was not made. The quantum yield for a $O(^3P) + O_2(^1\Sigma_g^+)$ channel would have to be as high as 0.56 at $\lambda = 311$ nm to explain the observations[70]. What is clear, however, is that there is experimental support for the idea of a singlet molecular fragment being formed along with a triplet atom in the tail of the Hartley band. From the point of view of atmospheric chemistry, it may not even matter which singlet molecular state is formed, since at altitudes below about 70 km quenching by $N_2$ is the most probable fate of $O_2(^1\Sigma_g^+)$, and the product of quenching is believed to be $O_2(^1\Delta_g)$[75].

The direct or indirect production of $O_2(^1\Delta_g)$ at $\lambda > 310$ nm needs to be considered if IR atmospheric band intensities are to be used to estimate ozone concentrations in the lower stratosphere and below[84]. Long-wavelength photolysis is likely to show the largest influence for large solar zenith angles and at low altitudes.

## Vibrationally excited oxygen from ozone photolysis

Even relatively modest experiments have been used to look at the products on a time scale short enough that vibrational relaxation has not wiped out more detailed information. Klais *et al.*[85] were able to use flash photolysis, followed by absorption in the vacuum ultraviolet region, to study vibrationally excited $O_2(^1\Delta_g)$. The experiments not only provide further confirmation that $O_2(^1\Delta_g)$ is a primary product of photolysis, but also give an idea of the partitioning into the accessible vibrational levels. Time-of-flight photofragment spectroscopy provides even more detailed information. For example, Sparks *et al.*[60] used the product energy information in conjunction with polarization dependence data to show that the relative yields of photolysis at $\lambda = 266$ nm into $v' = 0$, 1, 2 and 3 of $O_2(^1\Delta_g)$ are 0.57, 0.24, 0.12, and 0.07.

Coherent anti-Stokes Raman spectroscopy (CARS) has been employed by Valentini and co-workers to investigate dissociation of ozone in the Chappuis[71,72] and Hartley[69,70] absorption regions. CARS is a multiphoton spectroscopy dependent on nonlinear effects resulting from the use of high-intensity lasers. Very high time resolution is inherent in the technique, because the time scale is that of the Raman process itself, and the true nascent molecular oxygen photofragments are probed. In the Chappuis region, vibrational levels in $O_2(^3\Sigma_g^-)$ up to $v = 4$ are seen and the vibrational distribution remains virtually the same for photolysis from $\lambda = 560$ to 638 nm, even though at the longest wavelength $v = 4$ is the highest accessible vibrational level, while at the shortest $v = 6$ could be

populated. One interesting observation is a small population inversion between $v=3$ and $v=2$ at all wavelengths. The constancy of the distribution indicates that the dissociation is vibrationally adiabatic, with the exit channel dynamics being involved only in the partitioning of energy between rotational and translational modes. Simple kinematics explain[72] the vibrational adiabaticity. Because the equilibrium bond angle in $O_3$ is quite small (ca. 117°), the repulsive impulse between the photofragments has a small projection along the O–O bond in the $O_2$ product. Only about five per cent of the available energy could appear as vibration even if the interaction were purely impulsive[71]. Appreciable rotational excitation is expected to follow repulsion of O from $O_2$ because of the small bond angle, and such excitation is, indeed, seen.

CARS spectra have been obtained[70] at 17 different wavelengths in the Hartley band. At each photolysis wavelength, all energetically accessible vibrational states are populated (with $v$ up to 7 for photolysis at $\lambda=230$ nm), in contrast to the behaviour for photolysis by visible radiation described above. Nevertheless, the most probable vibrational state is always $v=0$, and the vibrational distribution is nearly independent of photolysis wavelength, apart from the population of the higher vibrational levels of $O_2(^1\Delta_g)$ at the shorter wavelengths. Figure 2 shows the spectrum for photolysis at $\lambda=240$ nm. One most remarkable feature of these CARS spectra concerns the *rotational* distributions, and we shall return to this aspect in the next section. For the moment, we note that even though high-$J$ rotational states are produced, conservation of angular momentum prevents a large fraction of the available energy from appearing as rotation. Thus, since $v=0$ predominates in the vibrational distribution, most of the energy difference between the photon energy and that needed to form $O(^1D)+O_2(^1\Delta_g)$ appears as translation. Figure 3 shows the good agreement between the CARS measurements of vibrational state distributions for photolysis at $\lambda=266$ nm and those obtained by photofragment time-of-flight spectroscopy[60] at the same wavelength. Initial bond lengths in the $^1A_1$ state of $O_3$ and in the $^1\Delta_g$ state of $O_2$ are not much different, so that vibrational excitation is not expected from the Franck–Condon overlap of reactant and product. However, the upper state of the Hartley system ($1^1B_2$) has a calculated[14] bond length of 1.405 Å, as against 1.271 Å for the ground state of $O_3$. The relative lack of vibrational excitation must therefore mean that the gradients on the potential energy surface are sufficient to drive the dissociating system out of the Franck–Condon region so rapidly that there is no time to excite the preserved O–O bond.

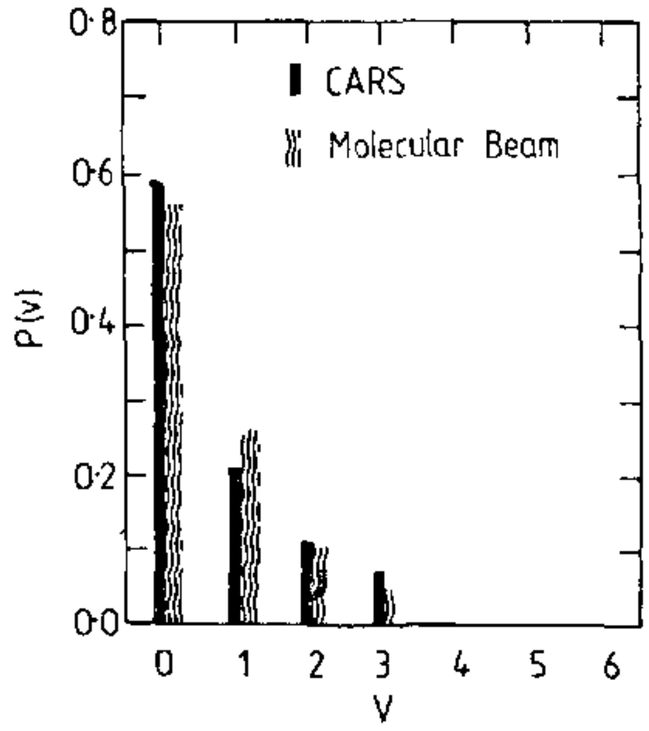


**Figure 3.** Vibrational state distributions in the $O_2(^1\Delta_g)$ fragment of photolysis of ozone at $\lambda=266$ nm obtained by CARS[70] and time-of-flight[60] techniques. Reproduced from ref. 70.

Vibrational energy release in the minor channel of the Hartley-band dissociation to yield $O(^3P)+O_2(^3\Sigma_g^-)$ is implicit in the various photofragmentation experiments[60–62]. In the most recent of these[62], REMPI detection was coupled with both time-of-flight spectroscopy and high-resolution Doppler profile measurements on the $O(^3P)$ fragments. The recovered translational energy distribution is sufficiently well resolved for the vibrational distribution in $O_2$ to be inferred. Excitation is seen up to beyond $v=20$, with a maximum (and mean) at roughly $v=12$ to 15, as indicated in Figure 4. It should be noted that a rotational temperature is needed to obtain the vibrational distribution, and the value adopted by Kinugawa *et al.*[62] is based on an impulsive model of ozone dissociation[86]. Angular distributions were probed in these experiments by measuring the spectra as a function of the angle between the polarization vector of the dissociation laser and the detector axis. The anisotropy factor that is derived gives information about the dissociation lifetime, which is dependent on the time taken for the wave packet prepared on the upper surface of the Hartley system to reach the seam of the predissociating potential surface (see Figure 1 for a two-dimensional representation of some calculated

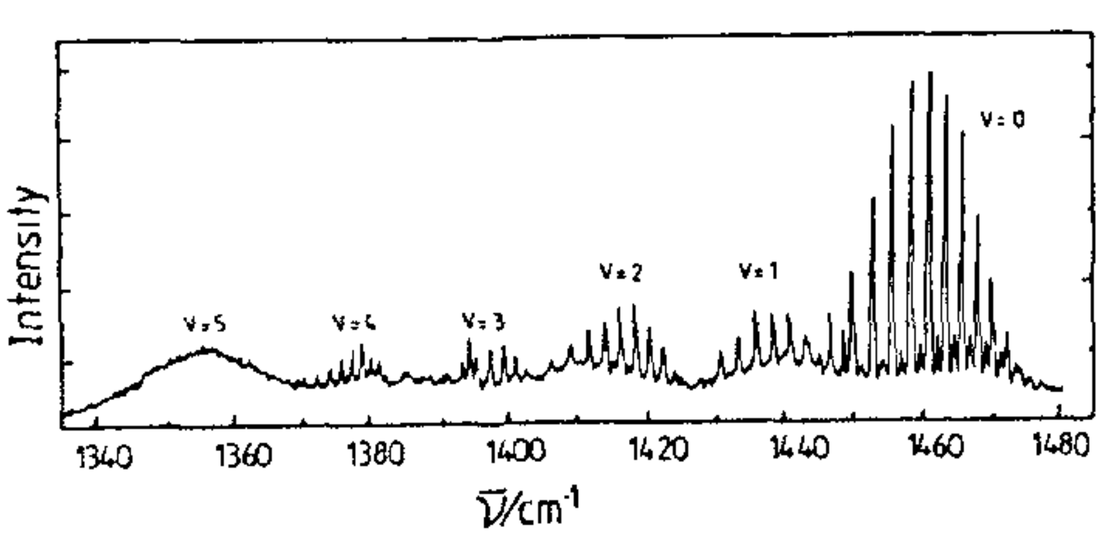


**Figure 2.** Coherent Raman anti-Stokes spectrum (vibrational $Q$ branch) of $O_2(^1\Delta_g)$ produced in the photolysis of ozone at $\lambda=240$ nm. Note the alternation in intensities between neighbouring $J$ levels. Reproduced from ref. 70.

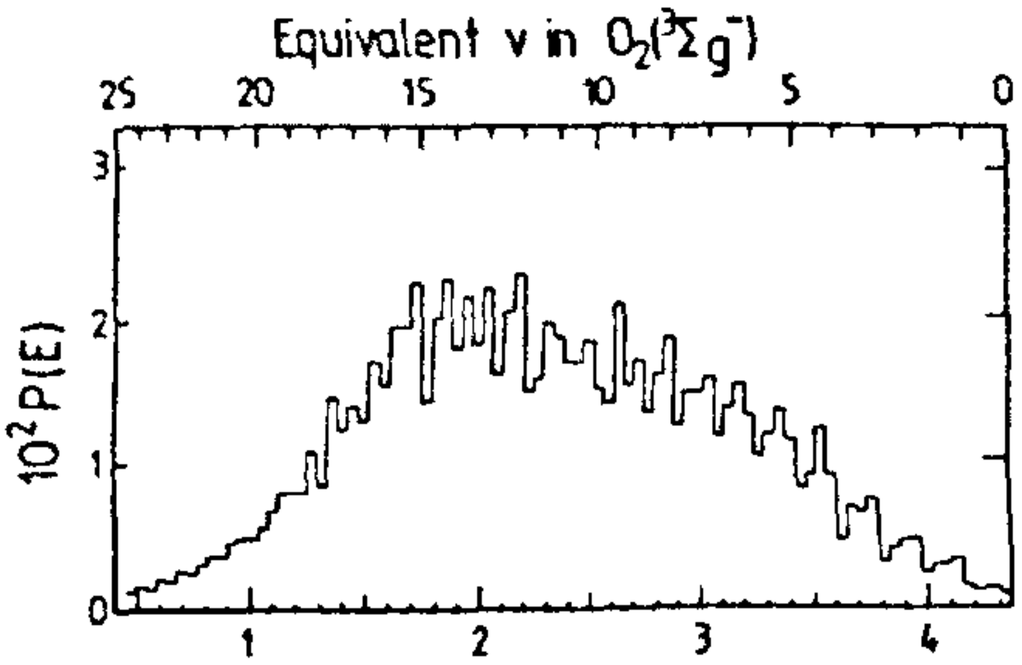


**Figure 4.** Translational energy distribution[62] function, $P(E)$, of $O(^3P)$ fragments from the photodissociation of ozone at $\lambda = 226.06$ nm. The vibrational quantum states in ground-state $O_2$ are indicated. A rotational temperature of 4000 K is assumed in deriving the distribution.

surfaces). According to one set of calculations[87], this evolution time is 10 fs, and the excitation of the product $O_2$ is a consequence of the extended geometry reached at this time. A simple relationship for a harmonic oscillator[62] predicts an averaged vibrational level of 11, in good agreement with the experimental value of 14.

The inference of high degrees of vibrational excitation in the minor channel of ozone photodissociation in the Hartley band is of particular interest in relation to upper stratospheric and mesospheric ozone densities. Slanger *et al.*[88] showed ozone could be generated with $\lambda = 248$ nm laser radiation incident on $O_2$, even though at this wavelength there is insufficient energy to dissociate molecular oxygen. The key feature of the solution proposed by Slanger *et al.*[88] was that photodissociation of $O_3$ led to vibrationally excited $O_2$ as just described, and that this excited $O_2$ *is* capable of being dissociated at the laser wavelength. Slanger *et al.* went on to speculate that a process of this kind, which ultimately is capable of yielding three oxygen atoms (and thus three ozone molecules) for each molecule of ozone photolysed, might be of atmospheric importance. There is a need for such a mechanism, since most models of upper stratospheric and mesospheric ozone photochemistry underestimate the amount of ozone present. The quantitative experimental data of Kinugawa *et al.*[62] now permit incorporation of these ideas into atmospheric models. Toumi *et al.*[5] show that the enhanced production of odd oxygen with the new source allows model and observations to be reconciled. As an additional piece of evidence for the importance of vibrationally excited oxygen, these workers show that the observed enhancement of infrared emission from water vapour could be explained by energy transfer from excited $O_2$ to $H_2O$.

## Rotational energies and the dissociating molecule

Although the motivation of most of the laboratory investigations of nascent product energy distributions in the photolysis of ozone has been primarily that of understanding the photodissociation dynamics, it has nevertheless emerged that the results, even at the detail of the disposal of energy into rotation, have applications to atmospheric problems. In this section, we consider experiments that probe the dissociation of ozone at the most intimate level, and present the results without overemphasizing the interpretations of dynamics. Our remarks in this section are confined to photodissociation in the ultraviolet region.

Possibly the most remarkable feature of the CARS studies of the photodissociation of ozone in the ultraviolet region[69,70] is the rotational structure in the $O_2(^1\Delta_g)$ product. There is an anomalous propensity for even $J$, as indicated in Figure 2. Intensity alternations of this kind cannot be due to spectroscopic effects or nuclear degeneracy differences[69]. Rather, a dynamical bias in the photodissociation must be behind the alternations. Nuclear exchange symmetry restrictions allow only odd-$J$ levels in ground state $^{16}O\,^{16}O$ ($^3\Sigma_g^-$), because the nuclei have zero spin; in $O_2(^1\Delta_g)$, the situation is complicated by the existence of $\Lambda$-doubling, but again there are restrictions, even-$J$ levels being associated with the $\Delta^+$ components, and odd-$J$ with the $\Delta^-$ components. Nuclear-spin statistical effects might thus be a good place to look for an interpretation of the photodissociative behaviour. Valentini *et al.*[70] have carried out CARS photofragment spectroscopy on $O_2(^1\Delta_g)$ formed in the dissociation of isotopically substituted ozone. Both $^{16}O^{16}O$ and $^{18}O^{18}O$ products show the same propensity for even-$J$ rotational states, but the heteronuclear isotopomer $^{16}O^{18}O$ does not. Comparisons of the relative populations for $^{16}O^{18}O$ and $^{16}O^{16}O$ rotational levels demonstrate clearly that it is the odd-$J$ levels in the homonuclear isotope that are depleted relative to the even-$J$ levels, rather than the even-$J$ levels that are preferentially populated. This result thus excludes an explanation that calls for a preference in the photodissociation for the $\Delta^+$ $\Lambda$-doublet components of $O_2(^1\Delta_g)$. The data are, however, consistent with a preferential removal of the odd-$J$ levels in the curve-crossing process discussed earlier. It was pointed out then that there is a considerable body of evidence for about 10 per cent of the photolysis of ozone in the Hartley region resulting in the formation of two triplet products, $O(^3P) + O_2(^3\Sigma_g^-)$, by means of a radiationless energy transfer process. Figure 1 was used to illustrate the principle with reference to diatomic-like potential energy curves calculated for the ozone molecule[25]. Crossing is assumed to occur at large enough internuclear distances that the system behaves as separate atomic and diatomic species. Radiationless

transitions require that the parity of the two states involved should be the same, and thus that $J$ remain unchanged, or change by an even number of quanta. Because the level to which transfer is to occur, effectively $O_2(^3\Sigma_g^-)$, has only odd-$J$ levels available, transfer is possible only from odd-$J$ levels of $O_2(^1\Delta_g)$. Relative to these odd levels, therefore, there is an apparent propensity for the even-$J$ levels in the $O_2(^1\Delta_g)$ channel that remains. Here we observe a striking effect on nascent populations that arises from the dynamics of photodissociation coupled with quantum-spin effects.

The results just described are not only fascinating for the light they shed on the dynamics of dissociation but the phenomena may also have chemical and atmospheric consequences. One of these consequences concerns enrichment of stratospheric ozone in the isotope $^{18}O$, first suggested by Cicerone and McCrumb[89]. Subsequent experiments[90–93] have confirmed this idea, with the most recent[93] measurements suggesting an enrichment in $^{50}O_3$ that is 12–16 per cent in the altitude range 26–35 km and that increases with altitude. The isotope $^{17}O$ is apparently also enriched to roughly the same extent. It seems that the isotopic anomaly in ozone can even be transferred to $CO_2$ in the atmosphere[94], possibly through the addition of $O(^1D)$ to form a transient $CO_3$ species[95]. Laboratory studies, notably by Thiemens and co-workers[96], show that ozone can become isotopically enriched in a variety of sources. Valentini[97] has suggested that the interpretation of the isotopic enrichment may be sought in the rotational propensity observed in the nascent products of photolysis. The preference for even-$J$ rotational quantum states in the $O_2(^1\Delta_g)$ fragment is ascribed to a relative depopulation of the odd-$J$ levels, as just explained. Since the nuclei in $^{18}O^{16}O$ or in $^{17}O^{16}O$ are not equivalent, there are no symmetry restrictions, in agreement with the observed absence[70] of a propensity for odd- or even-$J$ in $^{18}O^{16}O(^1\Delta_g)$. Valentini[97] gives detailed consideration to how the observed isotope effects might lead to isotopic enrichment in both the laboratory and the atmospheric systems. However, this explanation is not universally accepted, since some of the more recent laboratory studies[98,99] seem to indicate isotopic enrichment even where only groundstate reactants are present[100], and other explanations for the observed effects in $O_3$ and $CO_2$ have been advanced[101].

We now return to the dynamics of the photodissociation of ozone. The general features of the rotational distributions make it clear that vibrationally adiabatic, rotationally impulsive energy release must dominate the dissociation. However, there are changes[70] of vibrational and rotational populations with wavelength, so that the energy release cannot be perfectly impulsive. The agreement between prediction of the most populated rotational level by the impulsive model and experiment is not perfect, even when allowance is made for the rotation and zero-point vibrational energy of the initial ozone reactant. Nevertheless, the width and shape of the rotational distributions can be well matched by the calculations. One essential component of the calculations is the incorporation of a vector correlation that requires the rotational angular momentum of the $O_2$ fragment derived from the in-plane rotation of the $O_3$ to be parallel to the angular momentum induced by the impulsive release of dissociation energy.

Yet more detailed information about the dynamics of dissociation requires a study of the ozone molecule while it is in the process of falling apart: that is, on a time scale of a few femtoseconds. Experiments conducted in *frequency*, rather than *time*, space[4,102] are able to examine processes on this time scale. Weak emission can be observed even from molecules that photodissociate if a high enough intensity of illumination is used. The emission process can be considered either as fluorescence or as resonantly enhanced Raman scattering; the point of consequence is that the emitted photons refer to the shortest possible time scale, while the two photofragments are still close to each other. Thus they probe the unbound potential surfaces on which dissociation occurs. Emission from the upper (dissociating) electronic state to discrete vibrational levels of the lower state reflects the projection of the time-evolving reaction onto the known vibrational wave functions of the ground electronic state. The frequencies of the fluorescence spectra are characteristic of the vibrational spacing of the electronic state from which absorption arises, while the intensities reflect the dynamics on the upper surface. Because the molecule is dissociating, it passes through infinite displacements, thus allowing effective Franck–Condon overlap over a wide range of lower-state vibrational levels. In the dissociation of ozone the initial equivalence of the two O–O bonds means that the dissociation involves the spreading of the wave packet on the upper surface. Observations of the emission have permitted characterization of the repulsive upper potential energy surface and of the dynamics of dissociation[4,102], as well as allowing investigation[24], via excitation spectroscopy, of the Huggins absorption spectrum. Figure 5 reproduces the photoemission spectrum obtained by Imre *et al.*[102] for excitation at $\lambda = 266$ nm. The spectrum consists of overtones and combination bands in $v_1$ (symmetric stretch) and even quanta in $v_3$ (antisymmetric stretch). No bands with $v_2 > 0$ (bending) are evident. As anticipated from the explanation of the emission process given in the preceding paragraphs, the vibrational progression in the fluorescence spectrum is unusually long. Vibrational levels of the ground, $^1A_1$, state of ozone are seen up to (700) at $\tilde{\nu} = 7523\ cm^{-1}$, which is within $500\ cm^{-1}$ of the energy of dissociation

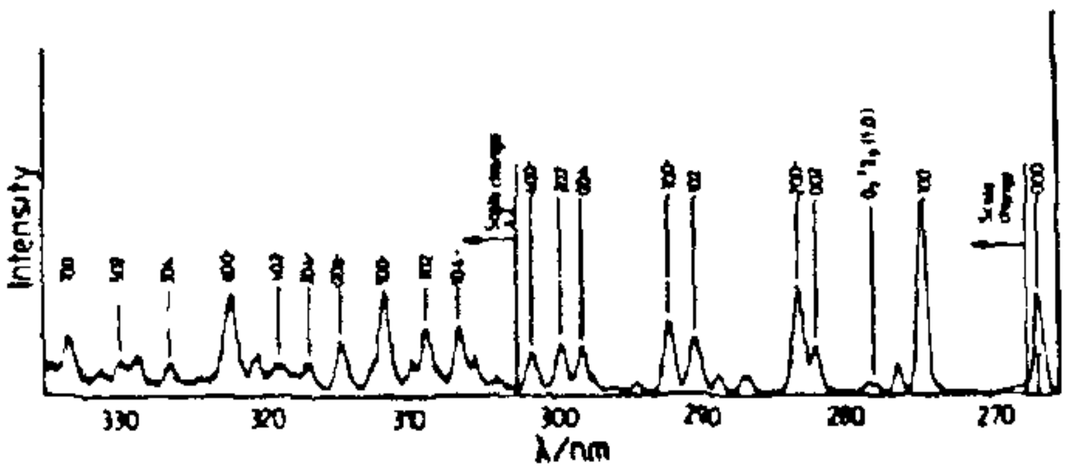


**Figure 5.** Photoemission spectrum[4] of $O_3$ excited at $\lambda = 266$ nm (resolution = 0.8 nm FWHM). The Raman fundamental of ground state $O_2$ appears weakly, and is labelled on the figure.

to $O(^3P) + O_2(^3\Sigma_g^-)$. The absence of $v_2$ activity suggests immediately that the bending mode is not much involved in the early stages of fragmentation. Thus the change in bond angle with excitation must be small, and both upper and lower surfaces must possess similar curvature with respect to the angle of bending. The relative intensities of the (100) and (002) bands yields quantitative information about the excited state, and demonstrates that the upper state potential has a maximum rather than a minimum with respect to the normal coordinate $q_3$ for the $v_3$ mode. The upper state is therefore better described as possessing $C_s$ rather than $C_{2v}$ symmetry, in agreement with several calculated potential surfaces[14,25]. The force along $q_3$ vanishes at the initial configuration of the wave packet, and a low intensity in this mode might be expected. However, rapid spreading of the wave packet along the $v_3$ mode permits the overtone transitions in this mode. The spreading motions maintain symmetry about the $C_{2v}$ axis. Odd quanta in $v_3$ are antisymmetric, and therefore vanish, leaving the observed even quanta.

Photodissociation itself starts by the transference of the wave packet to the excited state near the top of a saddle point along the $C_{2v}$ axis. The initial displacement from the energy minimum along $q_1$ leads to a rapid acceleration along the $q_1$ coordinate, and the generation of the long $v_1$ progression in emission. The absorption spectrum of ozone shows only very weak fine structure, which indicates that the wave packet does not revisit the Franck–Condon region many times before the irreversible motion in the $q_3$ coordinate[20,21,102]. Some information is thus provided about the rate of spread relative to the rate of motion along the symmetric stretch.

A considerable amount of theoretical work pertinent to the dynamics of photodissociation has been published recently. Further developments that are anticipated[4] include wavelength tuning to obtain further time resolution, higher-resolution spectroscopy, and accurate calculations of the motions of the wave packets on adjustable model surfaces to generate intensity distributions for comparison with experiment. Detailed analyses of the dynamics may ultimately provide the solutions to the remaining problems of ozone photochemistry that both physical chemists and atmospheric scientists await.

## Conclusions

This review has concentrated on just one aspect of ozone photochemistry, that of photodissociation. The research has a long history, but it is evident that much effort continues to be put into both experimental and theoretical aspects. Descriptions of photodissociation are becoming ever more sophisticated, and new puzzles are emerging. As the underlying physical chemistry has unfolded, so have new ideas become available for the interpretation of atmospheric phenomena. Alongside the work on photodissociation have been studies on other facets such as the vibrational photochemistry of ozone[8]. Vibrationally excited ozone molecules in the atmosphere are of interest for several reasons[103,104]; for example, they can exhibit a red shift in the ultraviolet absorption spectrum of ozone, they can show enhanced rates of photodissociation and reaction with other molecules, and they can produce infrared airglow from the atmosphere. Chemical reactions of vibrationally excited ozone are likely only in the mesosphere and above[103], but changes in absorption cross section and in quantum yield for $O(^1D)$ formation might be important at lower altitudes, especially for photolysis in the threshold wavelength region. Atmospheric measurements of infrared emission[103,105] from ozone are supplemented by laboratory experiments[104,106,107] that should help in the interpretation of the mesospheric and thermospheric processes that involve the species; testing of the concepts and models is eagerly anticipated[106]. Here, as in all other aspects of atmospheric chemistry, laboratory studies are seen to be the key to quantitative interpretation of the atmospheric phenomena; in turn, the atmospheric observations provide a powerful stimulus to exciting and innovative laboratory investigations.

1 Wayne, R. P., *Chemistry of Atmospheres*, Oxford University Press, Oxford, Second edition, 1991
2. Thomas, R. J., Barth, C. A., Rottman, G. J., Rusch, D. W., Mount, G. H., Lawrence, G. M., Sanders, R. W., Thomas, G. E. and Clemens, L. E., *Geophys Res. Lett.*, 1983, **10**, 245.
3. Thomas, R. J., Barth, C. A., Rusch, D. W and Sanders, R. W., *J. Geophys Res. (D)*, 1984, **89**, 9569
4 Imre, D G., Kinsey, J. L., Field, R. W and Katayama, D. H., *J. Phys. Chem.*, 1982, **86**, 2564
5. Toumi, R., Kerridge, B J. and Pyle, J. A., *Nature*, 1991, 351, 217.
6. Levine, R. D. and Bernstein, R. B., *Molecular Reaction Dynamics and Chemical Reactivity*, Oxford University Press, Oxford, 1987.
7. Wayne, R. P., *Atmos. Environ.*, 1987, **21**, 1683
8. Wayne, R P., in *Handbook of Environmental Chemistry* (ed

Hutzinger, O.), Springer–Verlag, Berlin, 1990, vol. 2, Part E, pp. 1–56.
9. Steinfeld, J. I., Adler–Golden, S. M. and Gallagher, J. W., JILA Data Center Report No. 31, 1987; *J. Phys. Chem. Ref. Data*, 1987, **16**, 911.
10. Katayama, D. H., *J. Chem. Phys.*, 1979, **71**, 815; *J. Chem. Phys.*, 1986, **85**, 6809.
11. Anderson, S. M., Morton, J. and Mauersberger, K., *J. Chem. Phys.*, 1990. **93**, 3826.
12. Vaida, V., Donaldson, D. J., Strickler, S. J., Stephens, S. L. and Birks, J. W., *J. Phys. Chem.*, 1989, **93**, 506.
13. Hay, P. J. and Dunning, T. H., Jr., *J. Chem. Phys.*, 1977, **67**, 2290.
14. Hay, P. J., Pack, R. T., Walker, R. B. and Heller, E. J., *J. Phys. Chem.*, 1982, **86**, 862.
15. Sheppard, M. G. and Walker, R. B., *J. Chem. Phys.*, 1983, **78**, 7191.
16. Adler–Golden, S. M., *J. Quant. Spectrosc. Radiat. Transfer.*, 1983, **30**, 175.
17. Atabek, O., Bourgeois, M. T. and Jacon, M., *J. Chem. Phys.*, 1986, **84**, 6699.
18. Johnson, B. R. and Kinsey, J. L., *J. Chem. Phys.*, 1989, **91**, 7638.
19. Le Quéré, F. and Leforestier, C., *J. Chem. Phys.*, 1990, **92**, 247.
20. Le Quéré, F. and Leforestier, C., *J. Chem. Phys.*, 1991, **94**, 1118.
21. Farantos, S. C. and Taylor, H. S., *J. Chem. Phys.*, 1991, **94**, 4887.
22. Tannor, D. J., *J. Am. Chem. Soc.*, 1989, **111**, 2772.
23. Brand, J. C. D., Cross, K. J. and Hoy, A. R., *Can. J. Phys.*, 1978, **56**, 327.
24. Sinha, A., Imre, D., Goble, J. H., Jr., and Kinsey, J. L., *J. Chem. Phys.*, 1986, **84**, 6108.
25. Banichevich, A., Peyerimhoff, S. D. and Grein, F., *Chem. Phys. Lett.*, 1990, **173**, 1.
26. Thunemann, K. H., Peyerimhoff, S. D. and Buenker, R. J., *J. Mol. Spectrosc.*, 1978, **70**, 432.
27. Wilson, C. W. Jr. and Hopper, D. G., *J. Chem. Phys.*, 1981, **74**, 595.
28. Jones, R. O., *Phys. Rev. Lett.*, 1984, **52**, 2002.
29. Jones, R. O., *J. Chem. Phys.*, 1985, **82**, 325.
30. Morin, M., Foti, A. E. and Salahub, D. R., *Can. J. Chem.*, 1985, **63**, 1982.
31. Stanton, J. F., Bartlett, R. J., Magers, D. H. and Lipscomb, W. N., *Chem. Phys. Lett.*, 1989, **163**, 333.
32. Lee, T. J., *Chem. Phys. Lett.*, 1990, **169**, 529.
33. Johnstone, W. M., Mason, N. J., Newell, W. R, Biggs, P., Marston, G. and Wayne, R. P., *J. Phys. B.*, 1992, (in press).
34. Shi, J. and Barker, J. R., *J. Phys. Chem.*, 1990, **94**, 8390.
35. Swanson, N. and Celotta, R. J., *Phys. Rev. Lett.*, 1975, **35**, 783.
36. McGrath, W. D., Maguire, J. M., Thompson, A., Trocha–Grimshaw, *Chem. Phys. Lett.*, 1983, **102**, 59; McGrath, W. D., Thompson, A. and Trocha–Grimshaw, *Planet. Space Sci.*, 1986, **34**, 1147.
37. von Rosenberg, C. W., Jr., and Trainor, D. W., *J. Chem. Phys.*, 1974, **61**, 2442; *J. Chem. Phys.*, 1975, **63**, 5348.
38. Wraight, P. C., *Planet. Space Sci.*, 1977, **25**, 1177.
39. Kleindienst, T., Locker, J. R. and Bair, E. J., *J. Photochem.*, 1980, **12**, 67.
40. Locker, J. R., Joens, J. A. and Bair, E. J., *J. Photochem.*, 1987, **36**, 235.
41. Ramirez, J. E., Bera, R. K. and Hanrahan, R. J., *Radiat. Phys. Chem.*, 1984, **23**, 685.
42. Norrish, R. G. W. and Wayne, R. P., *Proc. R. Soc. London, Ser. A*, 1965, **288**, 200.
43. Norrish, R. G. W. and Wayne, R. P., *Proc. R. Soc. London, Ser. A.*, 1965, **288**, 361.
44. Wayne, R. P., *Faraday Disc. Chem. Soc.*, 1972, **53**, 172.
45. Lee, L. C., Black, G., Sharpless, R. L. and Slanger, T. G., *J. Chem. Phys.*, 1980, **73**, 256.
46. Taherian, M. R. and Slanger, T. G., *J. Chem. Phys.*, 1985, **83**, 6246.
47. Arnold, I., Comes, F. J. and Moortgat, G. K., *Chem. Phys.*, 1977, **24**, 211.
48. Brock, J. C. and Watson, R. T., *Chem. Phys.*, 1980, **46**, 477.
49. Cobos, C., Castellano, E. and Schumacher, H. J., *J. Photochem.*, 1983, **21**, 291.
50. Fairchild, P. W. and Lee, E. K. C., *Chem. Phys. Lett.*, 1978, **60**, 36.
51. Kajimoto, O. and Cvetanovic, R. J., *Int. J. Chem. Kin.*, 1979, **11**, 605.
52. Moortgat, G. K. and Warneck, P., *Z. Naturforsch.*, 1975, **30a**, 835.
53. Philen, D. L., Watson, R. T. and Davis, D. D., *J. Chem. Phys.*, 1977, **67**, 3316.
54. Moortgat, G. K. and Kudszus, E., *Geophys. Res. Lett.*, 1978, **5**, 191.
55. Simons, J. W., Paur, R. J., Webster, H. A., III, Bair, E. J., *J. Chem. Phys.*, 1973, **59**, 1203.
56. Adler-Golden, S. M., Schweitzer, E. L. and Steinfeld, J. I., *J. Chem. Phys.*, 1982, **76**, 2201.
57. Astholz, D. C., Croce, A. E. and Troe, J., *J. Phys. Chem.*, 1982, **86**, 696.
58. Moortgat, G. K., Kudszus, E. and Warneck, P., *J. Chem. Soc. Faraday Trans. 2*, 1977, **73**, 1216.
59. DeMore, W. B., Molina, M. J., Sander, S. P., Golden, D. M., Hampson, R. F., Kurylo, M. J., Howard, C. J. and Ravishankara, A. R., Chemical Kinetics and Photochemical Data for use in Stratospheric Modeling, Evaluation Number 9, NASA, Washington, DC, 1990.
60. Sparks, R. K., Carlson, L. R., Shobatake, K., Kowalczyk, M. L. and Lee, Y. T., *J. Chem. Phys.*, 1980, **72**, 1401.
61. Fairchild, C. E., Stone, E. J. and Lawrence, G. M., *J. Chem. Phys.*, 1978, **69**, 3632.
62. Kinugawa, T., Sato, T., Arikawa, T., Matsumi, Y. and Kawasaki, M., *J. Chem. Phys.*, 1990, **93**, 3289.
63. Amimoto, S. T., Force, A. P., Wiesenfeld, J. R. and Young, R. H., *J. Chem. Phys.*, 1980, **73**, 1244.
64. Greenblatt, G. D. and Wiesenfeld, J. R , *J. Chem. Phys.*, 1983, **78**, 4924.
65. Brock, J. C. and Watson, R. T., *Chem. Phys. Lett.*, 1980, **71**, 371.
66. Wine, P. H. and Ravishankara, A. R., *Chem. Phys.*, 1982, **69**, 365.
67. Trolier, M. and Wiesenfeld, J. R., *J. Geophys. Res.*, 1988, **93**, 7119.
68. Turnipseed, A. A., Vaghjiani, G. L., Gierczak, T., Thompson, J. E. and Ravishankara, A. R., *J. Chem. Phys.*, 1991, **95**, 3244.
69. Valentini, J. J., *Chem. Phys. Lett.*, 1983, **96**, 395.
70. Valentini, J. J., Gerrity, D. R , Phillips, D. L., Nieh, J. -C. and Tabor, K. D., *J. Chem. Phys.*, 1987, **86**, 6745.
71. Moore, D. S., Bomse, D. S. and Valentini, J. J., *J. Chem. Phys.*, 1983, **79**, 1745.
72. Levene, H. B., Nieh, J. -C. and Valentini, J. J., *J. Chem. Phys.*, 1987, **87**, 2583.
73. Castellano, E. and Schumacher, H. J., *Z. Phys. Chem.*, 1962, NF**34**, 198.
74. Tkachenko, S. N., Zhuraviev, V. E., Popovich, M. P., Zhitnev, Yu. N. and Filippov, Yu. V., *Russ. J. Phys. Chem.*, 1980, **54**, 1304.
75. Wayne, R. P., in *Singlet Molecular Oxygen*, (ed. Frimer, A. A.), CRC Publishing Co., Boca Raton, Florida, 1985, vol. I, pp. 81–175.
76. Wayne, R. P., *J. Photochem.*, 1984, **25**, 345.
77. Huffman, R. E., Larrabee, J. C. and Barsley, V. C., *J. Chem. Phys.*, 1969, **50**, 4594.
78. Gauthier, M. and Snelling, D. R , *Chem Phys. Lett.*, 1970, **5**, 93.
79. Gauthier, M. and Snelling, D. R., *J. Chem Phys*, 1971, **54**, 4317.
80. Jones, I. T. N. and Wayne, R. P., *Proc. R. Soc. London, Ser. A*,

1971, 321, 409.
81. Castellano, F. and Schumacher, H. J., *Chem. Phys. Lett.*, 1972, 13, 625.
82. Jones, I. T. N. and Wayne, R. P., *J. Chem. Phys*, 1969, 51, 3617.
83. Jones, I. T. N. and Wayne, R. P., *Proc. R. Soc. London, Ser. A.*, 1970, 319, 273.
84. Crutzen, P. J., Jones, I. T. N. and Wayne, R. P., *J. Geophys. Res.*, 1971, 76, 1490.
85. Klais, O., Laufer, A. H. and Kurylo, M. J., *J. Chem Phys.*, 1980, 73, 2696
86. Levene, H. B and Valentini, J. J., *J. Chem Phys.*, 1987, 87, 2594.
87. Chasman, D., Tannor, D. J. and Imre, D. G., *J. Chem. Phys.*, 1988, 86, 6667.
88. Slanger, T. G., Jusinski, L. E., Black, G. and Gadd, G. E., *Science*, 1988, 241, 945
89. Cicerone, R. J. and McCrumb, J. L., *Geophys. Res. Lett.*, 1980, 7, 251.
90. Mauersberger, K., *Geophys. Res. Lett.*, 1981, 8, 935.
91. Mauersberger, K., *Geophys. Res. Lett.*, 1987, 14, 80
92. Rinsland, C. P., Malathy Devi, V., Flaud, J. -M., Camy-Peyret, C., Smith, M. A. H. and Stokes, G. M., *J. Geophys. Res.*, 1985, 90, 10719.
93. Schueler, B., Morton, J. and Mauersberger, K., *Geophys. Res. Lett.*, 1990, 17, 1295.
94. Thiemens, M. H., Jackson, T., Mauersberger, K., Schueler, B. and Morton, J., *Geophys. Res. Lett.*, 1991, 18, 699.
95. Yung, Y. L., DeMore, W. B and Pinto, J. P., *Geophys. Res. Lett.*, 1991, 18, 13.
96. Wen, J. and Thiemens, M. H., *Chem Phys. Lett.*, 1990, 172, 416
97. Valentini, J. J., *J. Chem. Phys*, 1987, 86, 6757.
98. Morton, J., Schueler, B and Mauersberger, K., *Chem. Phys Lett.*, 1989, 154, 143.
99. Anderson, S. M., Morton, J. and Mauersberger, K., *Chem. Phys. Lett.*, 1989, 156, 175.
100. Morton, J., Barnes, J., Schueler, B. and Mauersberger, K., *J. Geophys. Res.*, 1990, 95, 901.
101. Bates, D. R., *J. Chem. Phys*, 1990, 93, 8739.
102. Imre, D., Kinsey, J. L., Sinha, A. and Krenos, J., *J. Phys. Chem*, 1984, 88, 3956.
103. Rawlins, W. T., *J. Geophys. Res.*, 1985, 90, 12283.
104. Rawlins, W. T. and Armstrong, R. A., *J. Chem. Phys*, 1987, 87, 5202.
105. Adler-Golden, S. R. and Smith, D. R., *Planet. Space Sci.*, 1990, 38, 1121.
106. Rawlins, W. T., Caledonia, G. E. and Armstrong, R. A., *J. Chem. Phys.*, 1987, 87, 5209.
107. Ménard-Bourcin, F., Ménard, J. and Doyenette, L., *J. Chem. Phys.*, 1991, 94, 1875.

# Ozone observations and research in New Zealand – A historical perspective

**E. Farkas**

80 Ranui Crescent, Wellington 4, New Zealand.

## Introduction

THIS paper is a summary of the ozone work carried out in New Zealand, mainly within the New Zealand Meteorological Service, during the last seven decades. Its main aim has been to link local research activities to the progression of many new ideas and discoveries reported internationally in atmospheric physics, chemistry and dynamics, particularly in the last four decades. Results of analysis of up-to-date series of total and Umkehr ozone observations made in New Zealand are also discussed.

## Early ozone projects in New Zealand, 1929–1960

### *Total ozone observations in 1929*

The earliest total ozone observations were carried out in New Zealand at Christchurch (43.5° S, 172.5° E) during August to November 1929 with a Fery spectrograph, as part of the first global ozone-monitoring network organized by Dobson from Oxford. The instrument was on loan for the duration of the experiment, and the photographic plates were evaluated at Oxford. Since in those days it was practically impossible to obtain copies of weather charts from distant places on a regular basis, Dobson had invited local meteorologists to contribute short discussions on the relationship of daily ozone variations with meteorological conditions in their own regions, to be included in the final publication of the network results. Kidson of the New Zealand Meteorological Service did so for the New Zealand observations[1], laying the foundations of interest in ozone research within the Meteorological Service.

### *Acquisition of Dobson spectrophotometer No. 17*

After a satisfactory commercial production of three prototypes of Dobson's 'new' photo-electric ozone spectrophotometer in the early thirties, building of a larger batch of 20 instruments was planned for 1936 at